Periodic four-dimensional solution for transport of intense and coupled coasting beams through quadrupole channels

C. Xiao and L. Groening

GSI Helmholtzzentrum für Schwerionenforschung GmbH, D-64291 Darmstadt, Germany

(Received 6 November 2023; accepted 4 March 2024; published 20 March 2024)

Imposing angular momentum to a particle beam increases its stability against perturbations from space charge [Y.-L. Cheon *et al.*, Phys. Rev. Accel. Beams **25**, 064002 (2022)]. In order to fully explore this potential, proper matching of intense coupled beams along regular lattices is mandatory. Herein, a novel procedure assuring matched transport is described and benchmarked through simulations. The concept of matched transport along periodic lattices has been extended from uncoupled beams to those with considerable coupling between the two transverse degrees of freedom. For coupled beams, matching means the extension of cell-to-cell periodicity from just transverse envelopes to the coupled beam moments and to quantities being derived from these.

DOI: 10.1103/PhysRevAccelBeams.27.031602

I. INTRODUCTION

Preservation of beam quality is of major concern for acceleration and transport, especially of intense hadron beams. This aim is reached at best through the provision of smooth and periodic beam envelopes, being so-called matched to the periodicity of the external focusing lattice. The latter is usually composed of a regular arrangement of solenoids or quadrupoles. For the time being, the quality of matching has been evaluated through the periodicity of spatial beam envelopes. This is fully sufficient as long as there is no coupling between the phase space planes (for brevity "planes"), neither in beam properties nor in lattice properties.

For beams without coupling, various matching methods for intense beams have been proposed and realized in operation. First approaches, being still applied nowadays, base on differential rms-envelope equations formulated by Sacherer [1,2]. These assume KV distributions and calculate space charge forces from homogeneously charged rms-equivalent ellipsoids. The forces are linear and preserve the rms emittances. Albeit assuming artificial KV distributions, rms-equivalent matching of real beams has been conducted very successfully during the last decades. It became a state-of-the-art tool in the operation of modern intense-beam accelerators, see [3–5] for instance. Proper periodic solutions are especially relevant for systematic optimization of different lattice properties with respect to preservation of beam quality. Usually, the lattice parameter being optimized is its focusing strength, i.e., the imposed phase advance.

Variation of lattice parameters revealed many tools to optimize acceleration of intense beams with given emittances and intensity. Focusing can be accomplished by solenoids or by quadrupoles and systematic comparisons are discussed in [6]. Another way is varying the phase advance along the periodic structure as considered in [7]. Already in 1960s, different quadrupole focusing schemes such as FODO, FOFODODO, and FOFOFODODODO have been analyzed systematically [8].

Recent studies revealed that introducing angular momentum to the incoming beam opens another set of free parameters for further optimizing beam quality along periodic lattices [9]. Evidence has been provided that beam stability against perturbations from nonlinear space charge forces increases with the amount of introduced angular momentum. This is in analogy to the stabilization of flying objects such as bullets or footballs through spinning.

Imposing angular momentum is a very promising tool to further augment accelerator performance. It causes coupling between the horizontal and vertical plane and thus implies dedicated efforts for proper matching to periodic lattices. Matching with coupling between the horizontal and longitudinal plane has been investigated in [10]. Beams acquire finite angular momentum through, i,e., the presence of skew quadrupole errors or longitudinal magnetic fields [11]. Special cases of beams with zero four-dimensional emittances have been treated in [12] (x-y coupling).

The present work is on the development and demonstration of a method to determine a solution for four-dimensional (4D) rms-matched transport of intense beams with considerable transverse coupling, an issue being addressed conceptually in [13]. It partially implements the early concept, i.e., tracking of moments, into a procedure to

obtain full cell-to-cell 4D-periodicity. Through simulations, it is shown that the lattice periodicity is not just matched by the two transverse envelopes but also by the beam rms moments that quantify coupling. To this end, an iterative procedure toward the periodic solution is applied. It starts by determining the solution with zero current, using a method that is applied later also to beams with current.

The TRACE-2D code [14] is well suited to provide for a matching beam line between a given initial beam matrix and a desired exit beam matrix even for a full 4D scenario. However, it is an intrinsic property of the periodic-solution-problem that the initial beam matrix at the entrance of the periodic channel is unknown. Accordingly, this code cannot be applied to the present scenario in a straightforward way.

It is explicitly stated here that providing for a specific design of the matching line itself is beyond the scope of the present work. This paper aims to demonstrate that a 4D-periodic cell-by-cell solution exists and demonstrates its derivation. A detailed definition of the specific matching line is a hard task to be addressed in future work. However, a tentative approach is sketched in the Appendix.

The following section briefly introduces basic terms of beam rms-moments transportation through linear lattice elements. Afterward, the beam line providing angular momentum, matching, and periodic focusing is introduced. The fourth section is on modeling the periodic channel for beams without and with current, followed by the description of the procedure to determine the fully 4D-periodic solution for intense coupled beams. Maintenance of periodic solution along the quadrupole channel is discussed in the fifth section. Finally, benchmarking of the procedure to results obtained from tracking an intense coupled Gaussian beam using a well-established simulation code is presented. This includes also a comparison of the fully 4D-periodic solution with the solution from simple 2D-envelope matching with respect to their performance regarding suppression of 4D emittance growth.

II. BASIC CONCEPTS OF BEAM SECOND MOMENTS TRANSPORTATION

Particle coordinates are denoted by a 4×1 column vector $\vec{r}(s)$ with elements $x(s)$, $x'(s)$, $y(s)$, and $y'(s)$ with

$$u'(s) := \frac{du(s)}{ds}, \tag{1}$$

defining the derivation of the spatial coordinate u (refers to either x or y) with respect to the longitudinal coordinate s. It is assumed that the according transverse velocity $\beta c u'$ is small in comparison to the main propagation velocity βc of the beam along s. Linear transport of particle coordinates from an initial location to a final location is modeled through a linear 4×4 matrix equation

$$[\vec{r}(s)]_{\text{final}} := M \cdot [\vec{r}(s)]_{\text{initial}}. \tag{2}$$

Coupled beams inhabit ten independent second-order rms moments. They are summarized within the symmetric beam moments matrix

$$C := \begin{bmatrix} \langle xx \rangle & \langle xx' \rangle & \langle xy \rangle & \langle xy' \rangle \\ \langle x'x \rangle & \langle x'x' \rangle & \langle x'y \rangle & \langle x'y' \rangle \\ \langle yx \rangle & \langle yx' \rangle & \langle yy \rangle & \langle yy' \rangle \\ \langle y'x \rangle & \langle y'x' \rangle & \langle y'y \rangle & \langle y'y' \rangle \end{bmatrix} \tag{3}$$

and beam moments are transported through

$$C_{\text{final}} = M \cdot C_{\text{initial}} \cdot M^{\text{T}}. \tag{4}$$

Four of the elements of C quantify beam coupling. Beams are x-y coupled if at least one of these elements is different from zero. The projected rms emittances ε_x and ε_y are defined through the determinants of the two on-diagonal sub-matrices as

$$\varepsilon_u = \sqrt{\langle uu \rangle \langle u'u' \rangle - \langle uu' \rangle^2}, \tag{5}$$

i.e., they do not depend on coupled beam moments. In turn, the transverse eigenemittances [15]

$$\varepsilon_{1,2} = \sqrt{-\frac{\text{tr}[(CJ)^2]}{4} \pm \sqrt{\frac{\text{tr}^2[(CJ)^2]}{16} - \det(C)}} \tag{6}$$

and the 4D emittance is defined as

$$\varepsilon_{4\text{d}} = \sqrt{\det(C)} = \varepsilon_1 \cdot \varepsilon_2 \tag{7}$$

depend on all beam second moments including those with coupling. Any linear transformation M obeying

$$J = M^{\text{T}} \cdot J \cdot M, \qquad J := \begin{bmatrix} 0 & 1 & 0 & 0 \\ -1 & 0 & 0 & 0 \\ 0 & 0 & 0 & 1 \\ 0 & 0 & -1 & 0 \end{bmatrix}, \tag{8}$$

is called symplectic and preserves both eigenemittances. Just if M does not include any coupling elements, it will also preserve the projected rms emittances. In case a transformation M decouples a given beam, the decoupled beam's rms emittances are equal to the transverse eigenemittances that remain unchanged by M. Coupling can be quantified by the coupling parameter [16]

$$t := \frac{\varepsilon_x \cdot \varepsilon_y}{\varepsilon_{4\text{d}}} - 1, \tag{9}$$

and if and only if t is equal to zero, there is no interplane correlation and the projected rms emittances are equal to the eigenemittances.

Coupling is introduced by solenoids and rotated quadrupoles. A solenoid of length L shall have the longitudinal magnetic field strength B along the positive beam direction. The solenoid's strength is defined by $K \coloneqq B/2(B\rho)$. Additionally, we have $C \coloneqq \cos(KL)$ and $S \coloneqq \sin(KL)$. The solenoid transport matrix is

$$M_{\mathrm{sol}} = \begin{bmatrix} C^2 & \frac{SC}{K} & SC & \frac{S^2}{K} \\ -SCK & C^2 & -S^2K & SC \\ -SC & -\frac{S^2}{K} & C^2 & \frac{SC}{K} \\ S^2K & -SC & -SCK & C^2 \end{bmatrix}. \tag{10}$$

Although introducing coupling, solenoids preserve the beam angular momentum.

Quadrupoles instead, may change the amount of coupling as well as the angular momentum. The on-diagonal submatrices of a transport matrix M_{quad} of a regular quadrupole of strength $k \coloneqq GL/(B\rho)$ and effective length L are given by

$$Q_{xx} = \begin{bmatrix} \cos(kL) & \frac{\sin(kL)}{k} \\ -k\sin(kL) & \cos(kL) \end{bmatrix}, \tag{11}$$

and

$$Q_{yy} = \begin{bmatrix} \cosh(kL) & \frac{\sinh(kL)}{k} \\ k\sinh(kL) & \cosh(kL) \end{bmatrix}, \tag{12}$$

with G being the magnetic field gradient inside the quadrupole implying $B_y = Gx$ and $B_x = -Gy$. For positive (negative) G, quadrupoles focus in the horizontal (vertical) plane and defocus in the vertical (horizontal) plane. The coupling submatrices are zero.

The on-diagonal submatrices of a drift (M_{drift}) are

$$D_{xx} = D_{yy} = \begin{bmatrix} 1 & L \\ 0 & 1 \end{bmatrix}, \tag{13}$$

with its coupling submatrices being equal to zero. Finally, clockwise rotation of the beam by θ around the positive s axis is modeled through the symplectic matrix

$$R(\theta) = \begin{bmatrix} \cos(\theta) & 0 & -\sin(\theta) & 0 \\ 0 & \cos(\theta) & 0 & -\sin(\theta) \\ \sin(\theta) & 0 & \cos(\theta) & 0 \\ 0 & \sin(\theta) & 0 & \cos(\theta) \end{bmatrix}. \tag{14}$$

III. BEAM LINE FOR COUPLING, MATCHING, AND TRANSPORTATION

The beam line being used to determine the periodic solution of an intense coupled beam along a periodic channel is sketched systematically in Fig. 1. It comprises three sections, starting with a section that imposes coupling to the beam. It comprises five rotated quadrupoles and four solenoids being followed by a generic matching section. This section transports the beam parameters from the coupling section exit to the entrance of the periodic quadrupole channel. These two sections include coupling elements. The third section is a periodic sequence of noncoupling regular quadrupoles.

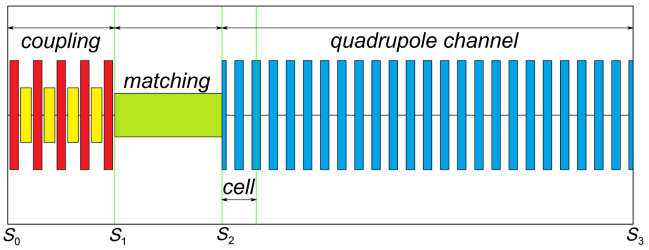

FIG. 1. The beam line comprises three parts: (I) coupling production section; (II) matching section; (III) regular quadrupole doublet section (12 cells). Red, yellow, and blue blocks indicate the rotated quadrupole, solenoid, and regular quadrupole, respectively. Space charge effects are not considered in the first two sections (see text).

At the beginning of the beam line, an uncoupled beam is assumed with beam sigma-matrix

$$C(s_0) = \begin{bmatrix} C_{xx} & O \\ O & C_{yy} \end{bmatrix}, \qquad O = \begin{bmatrix} 0 & 0 \\ 0 & 0 \end{bmatrix}, \tag{15}$$

the on-diagonal submatrices are

$$C_{xx} = \varepsilon_x \cdot \begin{bmatrix} \beta_x & -\alpha_x \\ -\alpha_x & \frac{1+\alpha_x^2}{\beta_x} \end{bmatrix}, \qquad C_{yy} = \varepsilon_y \cdot \begin{bmatrix} \beta_y & -\alpha_y \\ -\alpha_y & \frac{1+\alpha_y^2}{\beta_y} \end{bmatrix}, \tag{16}$$

and $\beta_u = \langle uu \rangle/\varepsilon_u$ and $\alpha_u = -\langle uu' \rangle/\varepsilon_u$. The beam matrix at the beginning of the matching section is calculated as

$$C(s_1) = \wp \cdot C(s_0) \cdot \wp^{\mathrm{T}}, \tag{17}$$

and $\wp$ indicates the transfer matrix of the coupling section.

In order to obtain a periodic solution for this beam, the details of the matching section are not required as seen in the following. However, it is modeled by a transport matrix including 16 elements (in units of m and rad)

$$\mathfrak{R}(\mathrm{m}_1, \mathrm{m}_2, \ldots, \mathrm{m}_{16}) = \begin{bmatrix} \mathrm{m}_1 & \mathrm{m}_2 & \mathrm{m}_3 & \mathrm{m}_4 \\ \mathrm{m}_5 & \mathrm{m}_6 & \mathrm{m}_7 & \mathrm{m}_8 \\ \mathrm{m}_9 & \mathrm{m}_{10} & \mathrm{m}_{11} & \mathrm{m}_{12} \\ \mathrm{m}_{13} & \mathrm{m}_{14} & \mathrm{m}_{15} & \mathrm{m}_{16} \end{bmatrix}. \tag{18}$$

Although initially being unknown, the 16 elements must ensure that $\mathfrak{R}$ is symplectic according to Eq. (8). For brevity, the set of $\mathtt{m}_1, \mathtt{m}_2, \ldots, \mathtt{m}_{16}$ shall be denoted by $\aleph$. The detailed layout of the matching section is beyond the scope of this paper. However, a conceptual approach is sketched in the Appendix.

The matching section is modeled through the symplectic and coupling matrix $\mathfrak{R}$ and hence

$$C(s_2) = \mathfrak{R} \cdot C(s_1) \cdot \mathfrak{R}^{\mathrm{T}} \tag{19}$$

is the beam matrix at the entrance to the quadrupole channel. The beam matrix at the exit of the first cell of the quadrupole channel is calculated as

$$C(s_2 + \ell) = \mathfrak{T} \cdot \mathfrak{R} \cdot C(s_1) \cdot (\mathfrak{T} \cdot \mathfrak{R})^{\mathrm{T}}. \tag{20}$$

The transport matrix of one cell has 16 elements

$$\mathfrak{T} = \begin{bmatrix} \mathtt{a}_1 & \mathtt{a}_2 & \mathtt{a}_3 & \mathtt{a}_4 \\ \mathtt{b}_1 & \mathtt{b}_2 & \mathtt{b}_3 & \mathtt{b}_4 \\ \mathtt{c}_1 & \mathtt{c}_2 & \mathtt{c}_3 & \mathtt{c}_4 \\ \mathtt{d}_1 & \mathtt{d}_2 & \mathtt{d}_3 & \mathtt{d}_4 \end{bmatrix}, \tag{21}$$

and the beam matrix at the entrance of the quadrupole channel has ten independent moments

$$C(s_2) = \begin{bmatrix} \mathtt{x}_1 & \mathtt{x}_2 & \mathtt{z}_1 & \mathtt{z}_2 \\ \cdots & \mathtt{x}_3 & \mathtt{z}_3 & \mathtt{z}_4 \\ \cdots & \cdots & \mathtt{y}_1 & \mathtt{y}_2 \\ \cdots & \cdots & \cdots & \mathtt{y}_3 \end{bmatrix}. \tag{22}$$

Accordingly, the analytical periodic solution of one cell meets the subsequent ten equations:

$$\begin{cases} \mathtt{x}_1 = \mathtt{a}_1^2\mathtt{x}_1 + 2\mathtt{a}_1\mathtt{a}_2\mathtt{x}_2 + \mathtt{a}_2^2\mathtt{x}_3 + 2\mathtt{a}_1\mathtt{a}_3\mathtt{z}_1 + 2\mathtt{a}_1\mathtt{a}_4\mathtt{z}_2 + 2\mathtt{a}_2\mathtt{a}_3\mathtt{z}_3 + 2\mathtt{a}_2\mathtt{a}_4\mathtt{z}_4 + \mathtt{a}_3^2\mathtt{y}_1 + 2\mathtt{a}_3\mathtt{a}_4\mathtt{y}_2 + \mathtt{a}_4^2\mathtt{y}_3 \\ \mathtt{x}_2 = \mathtt{a}_1\mathtt{b}_1\mathtt{x}_1 + (\mathtt{a}_1\mathtt{b}_2 + \mathtt{a}_2\mathtt{b}_1)\mathtt{x}_2 + \mathtt{a}_2\mathtt{b}_2\mathtt{x}_3 + (\mathtt{a}_1\mathtt{b}_3 + \mathtt{a}_3\mathtt{b}_1)\mathtt{z}_1 + (\mathtt{a}_1\mathtt{b}_4 + \mathtt{a}_4\mathtt{b}_1)\mathtt{z}_2 + (\mathtt{a}_2\mathtt{b}_3 + \mathtt{a}_3\mathtt{b}_2)\mathtt{z}_3 \\ +(\mathtt{a}_2\mathtt{b}_4 + \mathtt{a}_4\mathtt{b}_2)\mathtt{z}_4 + \mathtt{a}_3\mathtt{b}_3\mathtt{y}_1 + (\mathtt{a}_3\mathtt{b}_4 + \mathtt{a}_4\mathtt{b}_3)\mathtt{y}_2 + \mathtt{a}_4\mathtt{b}_4\mathtt{y}_3 \\ \mathtt{x}_3 = \mathtt{b}_1^2\mathtt{x}_1 + 2\mathtt{b}_1\mathtt{b}_2\mathtt{x}_2 + \mathtt{b}_2^2\mathtt{x}_3 + 2\mathtt{b}_1\mathtt{b}_3\mathtt{z}_1 + 2\mathtt{b}_1\mathtt{b}_4\mathtt{z}_2 + 2\mathtt{b}_2\mathtt{b}_3\mathtt{z}_3 + 2\mathtt{b}_2\mathtt{b}_4\mathtt{z}_4 + \mathtt{b}_3^2\mathtt{y}_1 + 2\mathtt{b}_3\mathtt{b}_4\mathtt{y}_2 + \mathtt{b}_4^2\mathtt{y}_3 \end{cases} \tag{23}$$

$$\begin{cases} \mathtt{z}_1 = \mathtt{a}_1\mathtt{c}_1\mathtt{x}_1 + (\mathtt{a}_1\mathtt{c}_2 + \mathtt{a}_2\mathtt{c}_1)\mathtt{x}_2 + \mathtt{a}_2\mathtt{c}_2\mathtt{x}_3 + (\mathtt{a}_1\mathtt{c}_3 + \mathtt{a}_3\mathtt{c}_1)\mathtt{z}_1 + (\mathtt{a}_1\mathtt{c}_4 + \mathtt{a}_4\mathtt{c}_1)\mathtt{z}_2 + (\mathtt{a}_2\mathtt{c}_3 + \mathtt{a}_3\mathtt{c}_2)\mathtt{z}_3 \\ +(\mathtt{a}_2\mathtt{c}_4 + \mathtt{a}_4\mathtt{c}_2)\mathtt{z}_4 + \mathtt{a}_3\mathtt{c}_3\mathtt{y}_1 + (\mathtt{a}_3\mathtt{c}_4 + \mathtt{a}_4\mathtt{c}_3)\mathtt{y}_2 + \mathtt{a}_4\mathtt{c}_4\mathtt{y}_3 \\ \mathtt{z}_2 = \mathtt{a}_1\mathtt{d}_1\mathtt{x}_1 + (\mathtt{a}_1\mathtt{d}_2 + \mathtt{a}_2\mathtt{d}_1)\mathtt{x}_2 + \mathtt{a}_2\mathtt{d}_2\mathtt{x}_3 + (\mathtt{a}_1\mathtt{d}_3 + \mathtt{a}_3\mathtt{d}_1)\mathtt{z}_1 + (\mathtt{a}_1\mathtt{d}_4 + \mathtt{a}_4\mathtt{d}_1)\mathtt{z}_2 + (\mathtt{a}_2\mathtt{d}_3 + \mathtt{a}_3\mathtt{d}_2)\mathtt{z}_3 \\ +(\mathtt{a}_2\mathtt{d}_4 + \mathtt{a}_4\mathtt{d}_2)\mathtt{z}_4 + \mathtt{a}_3\mathtt{d}_3\mathtt{y}_1 + (\mathtt{a}_3\mathtt{d}_4 + \mathtt{a}_4\mathtt{d}_3)\mathtt{y}_2 + \mathtt{a}_4\mathtt{d}_4\mathtt{y}_3 \\ \mathtt{z}_3 = \mathtt{b}_1\mathtt{c}_1\mathtt{x}_1 + (\mathtt{b}_1\mathtt{c}_2 + \mathtt{b}_2\mathtt{c}_1)\mathtt{x}_2 + \mathtt{b}_2\mathtt{c}_2\mathtt{x}_3 + (\mathtt{b}_1\mathtt{c}_3 + \mathtt{b}_3\mathtt{c}_1)\mathtt{z}_1 + (\mathtt{b}_1\mathtt{c}_4 + \mathtt{b}_4\mathtt{c}_1)\mathtt{z}_2 + (\mathtt{b}_2\mathtt{c}_3 + \mathtt{b}_3\mathtt{c}_2)\mathtt{z}_3 \\ +(\mathtt{b}_2\mathtt{c}_4 + \mathtt{b}_4\mathtt{c}_2)\mathtt{z}_4 + \mathtt{b}_3\mathtt{c}_3\mathtt{y}_1 + (\mathtt{b}_3\mathtt{c}_4 + \mathtt{b}_4\mathtt{c}_3)\mathtt{y}_2 + \mathtt{b}_4\mathtt{c}_4\mathtt{y}_3 \\ \mathtt{z}_4 = \mathtt{b}_1\mathtt{d}_1\mathtt{x}_1 + (\mathtt{b}_1\mathtt{d}_2 + \mathtt{b}_2\mathtt{d}_1)\mathtt{x}_2 + \mathtt{b}_2\mathtt{d}_2\mathtt{x}_3 + (\mathtt{b}_1\mathtt{d}_3 + \mathtt{b}_3\mathtt{d}_1)\mathtt{z}_1 + (\mathtt{b}_1\mathtt{d}_4 + \mathtt{b}_4\mathtt{d}_1)\mathtt{z}_2 + (\mathtt{b}_2\mathtt{d}_3 + \mathtt{b}_3\mathtt{d}_2)\mathtt{z}_3 \\ +(\mathtt{b}_2\mathtt{d}_4 + \mathtt{b}_4\mathtt{d}_2)\mathtt{z}_4 + \mathtt{b}_3\mathtt{d}_3\mathtt{y}_1 + (\mathtt{b}_3\mathtt{d}_4 + \mathtt{b}_4\mathtt{d}_3)\mathtt{y}_2 + \mathtt{b}_4\mathtt{d}_4\mathtt{y}_3 \end{cases} \tag{24}$$

$$\begin{cases} \mathtt{y}_1 = \mathtt{c}_1^2\mathtt{x}_1 + 2\mathtt{c}_1\mathtt{c}_2\mathtt{x}_2 + \mathtt{c}_2^2\mathtt{x}_3 + 2\mathtt{c}_1\mathtt{c}_3\mathtt{z}_1 + 2\mathtt{c}_1\mathtt{c}_4\mathtt{z}_2 + 2\mathtt{c}_2\mathtt{c}_3\mathtt{z}_3 + 2\mathtt{c}_2\mathtt{c}_4\mathtt{z}_4 + \mathtt{c}_3^2\mathtt{y}_1 + 2\mathtt{c}_3\mathtt{c}_4\mathtt{y}_2 + \mathtt{c}_4^2\mathtt{y}_3 \\ \mathtt{y}_2 = \mathtt{c}_1\mathtt{d}_1\mathtt{x}_1 + (\mathtt{c}_1\mathtt{d}_2 + \mathtt{c}_2\mathtt{d}_1)\mathtt{x}_2 + \mathtt{c}_2\mathtt{d}_2\mathtt{x}_3 + (\mathtt{c}_1\mathtt{d}_3 + \mathtt{c}_3\mathtt{d}_1)\mathtt{z}_1 + (\mathtt{c}_1\mathtt{d}_4 + \mathtt{c}_4\mathtt{d}_1)\mathtt{z}_2 + (\mathtt{c}_2\mathtt{d}_3 + \mathtt{c}_3\mathtt{d}_2)\mathtt{z}_3 \\ +(\mathtt{c}_2\mathtt{d}_4 + \mathtt{c}_4\mathtt{d}_2)\mathtt{z}_4 + \mathtt{c}_3\mathtt{d}_3\mathtt{y}_1 + (\mathtt{c}_3\mathtt{d}_4 + \mathtt{c}_4\mathtt{d}_3)\mathtt{y}_2 + \mathtt{c}_4\mathtt{d}_4\mathtt{y}_3 \\ \mathtt{y}_3 = \mathtt{d}_1^2\mathtt{x}_1 + 2\mathtt{d}_1\mathtt{d}_2\mathtt{x}_2 + \mathtt{d}_2^2\mathtt{x}_3 + 2\mathtt{d}_1\mathtt{d}_3\mathtt{z}_1 + 2\mathtt{d}_1\mathtt{d}_4\mathtt{z}_2 + 2\mathtt{d}_2\mathtt{d}_3\mathtt{z}_3 + 2\mathtt{d}_2\mathtt{d}_4\mathtt{z}_4 + \mathtt{d}_3^2\mathtt{y}_1 + 2\mathtt{d}_3\mathtt{d}_4\mathtt{y}_2 + \mathtt{d}_4^2\mathtt{y}_3. \end{cases} \tag{25}$$

A. General case: Matrix $\mathfrak{T}$ includes coupling

For matched envelopes, their respective waists occur at the quadrupole centers, hence they do as well occur at the entrance to the periodic channel as

$$\mathtt{x}_2 = \frac{\mathtt{x}_1'}{2} = 0, \qquad \mathtt{y}_2 = \frac{\mathtt{y}_1'}{2} = 0. \tag{26}$$

In the following shall be assumed (and shown later on) that the matching section can provide for a beam with coupled moments $\mathtt{z}_2 = \mathtt{z}_3 = 0$ (beam is coupled in $x - y$ space) at the centers of the quadrupoles along the periodic channel. The matched beam moments are accordingly rephrased as

$$\begin{cases} \mathtt{x}_1 = \mathtt{a}_1^2\mathtt{x}_1 + \mathtt{a}_2^2\mathtt{x}_3 + 2(\mathtt{a}_1\mathtt{a}_3\mathtt{z}_1 + \mathtt{a}_2\mathtt{a}_4\mathtt{z}_4) \\ +\mathtt{a}_3^2\mathtt{y}_1 + \mathtt{a}_4^2\mathtt{y}_3 \\ \mathtt{x}_2 = \mathtt{a}_1\mathtt{b}_1\mathtt{x}_1 + \mathtt{a}_2\mathtt{b}_2\mathtt{x}_3 + (\mathtt{a}_1\mathtt{b}_3 + \mathtt{a}_3\mathtt{b}_1)\mathtt{z}_1 \\ +(\mathtt{a}_2\mathtt{b}_4 + \mathtt{a}_4\mathtt{b}_2)\mathtt{z}_4 + \mathtt{a}_3\mathtt{b}_3\mathtt{y}_1 + \mathtt{a}_4\mathtt{b}_4\mathtt{y}_3 = 0 \\ \mathtt{x}_3 = \mathtt{b}_1^2\mathtt{x}_1 + \mathtt{b}_2^2\mathtt{x}_3 + 2(\mathtt{b}_1\mathtt{b}_3\mathtt{z}_1 + \mathtt{b}_2\mathtt{b}_4\mathtt{z}_4) \\ +\mathtt{b}_3^2\mathtt{y}_1 + \mathtt{b}_4^2\mathtt{y}_3 \end{cases} \tag{27}$$

$$\begin{cases} z_1 = a_1c_1x_1 + a_2c_2x_3 + (a_1c_3 + a_3c_1)z_1 \\ +(a_2c_4 + a_4c_2)z_4 + a_3c_3y_1 + a_4c_4y_3 \\ z_2 = a_1d_1x_1 + a_2d_2x_3 + (a_1d_3 + a_3d_1)z_1 \\ +(a_2d_4 + a_4d_2)z_4 + a_3d_3y_1 + a_4d_4y_3 = 0 \\ z_3 = b_1c_1x_1 + b_2c_2x_3 + (b_1c_3 + b_3c_1)z_1 \\ +(b_2c_4 + b_4c_2)z_4 + b_3c_3y_1 + b_4c_4y_3 = 0 \\ z_4 = b_1d_1x_1 + b_2d_2x_3 + (b_1d_3 + b_3d_1)z_1 \\ +(b_2d_4 + b_4d_2)z_4 + b_3d_3y_1 + b_4d_4y_3 \end{cases} \quad (28)$$

$$\begin{cases} y_1 = c_1^2x_1 + c_2^2x_3 + 2(c_1c_3z_1 + c_2c_4z_4) \\ +c_3^2y_1 + c_4^2y_3 \\ y_2 = c_1d_1x_1 + c_2d_2x_3 + (c_1d_3 + c_3d_1)z_1 \\ +(c_2d_4 + c_4d_2)z_4 + c_3d_3y_1 + c_4d_4y_3 = 0 \\ y_3 = d_1^2x_1 + d_2^2x_3 + 2(d_1d_3z_1 + d_2d_4z_4) \\ +d_3^2y_1 + d_4^2y_3. \end{cases} \quad (29)$$

Using these prerequistes, a dedicated numerical routine varies the 16 elements $m_1, m_2, \ldots, m_{16}$ in order to provide for according ten moments $x_1, x_2, \ldots, y_3$. Equations (27)–(29) shall be fully met by the input beam matrix $C(s_2)$ and the coupled matching matrix $\mathfrak{T}$. Finally, it shall be mentioned that the expression for the 4D emittance simplifies to

$$\varepsilon_{4d} = \sqrt{z_1^2z_4^2 - x_2y_2z_1^2 - x_1y_1z_4^2 + x_1x_3y_1y_3}. \quad (30)$$

B. Special case: Matrix $\mathfrak{T}$ includes no coupling

In special cases, even with space charge, the effective transfer matrix $\mathfrak{T}$ includes no coupling terms, i.e.,

$$\mathfrak{T} = \begin{bmatrix} a_1 & a_2 & 0 & 0 \\ b_1 & b_2 & 0 & 0 \\ 0 & 0 & c_3 & c_4 \\ 0 & 0 & d_3 & d_4 \end{bmatrix}, \quad (31)$$

for this case shall be assumed that the matching section can provide for a beam with the coupled moments $z_1 = z_4 = 0$ (beam is upright in $x - y$ space). The matched moments turn into

$$\begin{cases} x_1 = a_1^2x_1 + a_2^2x_3 \\ x_2 = a_1b_1x_1 + a_2b_2x_3 = 0 \\ x_3 = b_1^2x_1 + b_2^2x_3 \end{cases} \quad (32)$$

$$\begin{cases} z_1 = a_1c_4z_2 + a_2c_3z_3 = 0 \\ z_2 = a_1d_4z_2 + a_2d_3z_3 \\ z_3 = b_1c_4z_2 + b_2c_3z_3 \\ z_4 = b_1d_4z_2 + b_2d_3z_3 = 0 \end{cases} \quad (33)$$

$$\begin{cases} y_1 = c_3^2y_1 + c_4^2y_3 \\ y_2 = c_3d_3y_1 + c_4d_4y_3 = 0 \\ y_3 = d_3^2y_1 + d_4^2y_3. \end{cases} \quad (34)$$

In consequence, the generic matching section can be described by or replaced by a sequence of regular quadrupoles. Conventional 2D-envelope matching methods vary the matrix of the matching section m_1, m_2, m_5, m_6 and $m_{11}, m_{12}, m_{15}, m_{16}$, i.e., the gradients of individual quadrupoles, in order to produce the proper ten beam moments $x_1, x_2, \ldots, y_3$ and the eight elements a_1, a_2, b_1, b_2, and c_3, c_4, d_3, d_4. Equations (32)–(34) shall be fully met by the input beam matrix $C(s_2)$ and the uncoupled transfer matrix $\mathfrak{T}$. In this case, the 4D emittance simplifies to

$$\varepsilon_{4d} = \sqrt{z_1^2z_4^2 - x_1y_3z_3^2 - x_3y_1z_2^2 + x_1x_3y_1y_3}. \quad (35)$$

IV. MODELING OF PERIODIC CHANNEL

For zero current, the effective focusing forces are given solely by the external lattice. The actual beam shape has no influence on them and therefore the periodic solution even for coupled beams may be found analytically.

For intense beams instead, defocusing space charge forces depend on the beam shape and orientation in real space. Actually, they depend also on the spatial distribution type. However, since modeling of space charge forces using rms-equivalent KV distributions proved to work very well for matching purposes, this approach is followed here as well.

In the following, an iterative method is described to determine the periodic solution for zero current. At first glance, it seems more complicated with respect to a straight analytical approach. However, it has the advantage of being applicable easily to obtain the periodic solution even with current.

A. Beam with zero current

The periodic solution meets the condition

$$C(s_2) = \mathfrak{T} \cdot C(s_2) \cdot \mathfrak{T}^{\mathrm{T}} \quad (36)$$

and the transport matrix from the exit of the solenoid s_1 to the exit of the first cell is

$$\mathfrak{V}(\aleph) = \mathfrak{T} \cdot \mathfrak{R}(\aleph), \quad (37)$$

where $\mathfrak{T}$ is fully known from the cell of the quadrupole channel.

From the first principles, neither the periodic solution is known nor are the elements $\aleph$ that provide for the according matching from the exit of the solenoid s_1 to the entrance of the channel s_2. The iterative procedure to obtain finally both, starts with a guessed initial set $\aleph^i$ that just meets the

condition of being symplectic. It will most likely not meet the condition of the periodic solution, i.e.,

$$\mathfrak{R}(\aleph^{\iota}) \cdot C(s_1) \cdot \mathfrak{R}^{\mathrm{T}}(\aleph^{\iota}) \neq \mathfrak{V}(\aleph^{\iota}) \cdot C(s_1) \cdot \mathfrak{V}^{\mathrm{T}}(\aleph^{\iota}), \quad (38)$$

hence the beam matrix in front of the channel is different from the one behind the first cell.

With the MATHCAD [17] routine *Minerr*, a set of matching matrix elements $\aleph^0$ for zero beam current can be found, such that the symplectic condition is met sharply together with providing periodicity. The routine is dedicated to solve an underdetermined system of equations with a defined set of boundary conditions, such that

$$\mathfrak{R}(\aleph^0) \cdot C(s_1) \cdot \mathfrak{R}^{\mathrm{T}}(\aleph^0) = \mathfrak{V}(\aleph^0) \cdot C(s_1) \cdot \mathfrak{V}^{\mathrm{T}}(\aleph^0). \quad (39)$$

The parameters of the initially (s_0) uncoupled beam and the beam line are shown in Tables I and II, respectively.

After transport through the coupling production section (in units of m and rad)

$$\wp = \begin{bmatrix} +0.221 & +1.002 & -0.305 & +0.956 \\ -0.604 & -0.237 & -0.458 & -0.030 \\ -0.230 & -0.964 & -0.342 & +1.130 \\ +0.459 & -0.019 & -0.558 & +0.226 \end{bmatrix}, \quad (40)$$

the beam matrix is (in units of mm and mrad)

$$C(s_1) = \begin{bmatrix} +133.6 & -8.578 & +1.232 & +34.39 \\ \cdots & +139.5 & +33.85 & +133.3 \\ \cdots & \cdots & +151.4 & +28.22 \\ \cdots & \cdots & \cdots & +154.1 \end{bmatrix}. \quad (41)$$

With $\aleph^0$ being determined, the periodic beam matrix at the beginning of the channel has been calculated as (in units of mm and mrad)

TABLE I. Parameters of the uncoupled beam at position s_0.

Parameters	Value	Unit
Mass	$1.672621924 \times 10^{-27}$	kg
Charge	$1.602176634 \times 10^{-19}$	C
Vacuum permittivity	$8.854187813 \times 10^{-12}$	Fm^{-1}
Light speed	2.99792458×10^{8}	ms^{-1}
Energy	150	keV
Current	10	mA
ε_x and ε_y	29.97 and 195.5	mm mrad
β_x and β_y	0.460 and 3.032	$\mathrm{m\,rad}^{-1}$
α_x and α_y	−0.233 and −0.782	rad

$$C^0(s_2) = \begin{bmatrix} +125.5 & 0 & +54.87 & +27.77 \\ \cdots & +77.71 & -8.058 & +117.1 \\ \cdots & \cdots & +46.70 & 0 \\ \cdots & \cdots & \cdots & +343.6 \end{bmatrix}, \quad (42)$$

and it is equal to $C^0(s_2 + \ell)$.

As for the case of an uncoupled beam, the periodic solution of the coupled beam features $\alpha_x = \alpha_y = 0$ as expected from the symmetry of the regular cell of the channel. However, the corresponding coupling parameters from combinations of other planes are different from zero due to interplane coupling. The zero current transport matrix of one cell is (in units of m and rad)

$$\mathfrak{T}(\aleph^0) = \begin{bmatrix} +0.321 & +1.203 & 0 & 0 \\ -0.745 & +0.321 & 0 & 0 \\ 0 & 0 & +0.321 & +0.349 \\ 0 & 0 & -2.569 & +0.321 \end{bmatrix}, \quad (43)$$

and evaluation of its subtraces delivers the zero current phase advance of $\mu_0 = 71.26°$.

TABLE II. Parameters of the simulated beam line including the coupling production section, matching section, and one periodic cell. The unit of strength of solenoid is T.

Elements	Length (cm)	Strength (T/m)	Rotation (°)
Drift	5		
Rotated quad	20	0.024	0.068
Drift	5		
Solenoid	25	0.075	
Drift	5		
Rotated quad	20	−0.291	0.192
Drift	5		
Solenoid	25	0.075	
Drift	5		
Rotated quad	20	0.372	−0.066
Drift	5		
Solenoid	25	0.075	
Drift	5		
Rotated quad	20	−0.261	2.854
Drift	5		
Solenoid	25	0.075	
Drift	5		
Rotated quad	20	0.126	1.220
Drift	5		
Matching section	Unknown	Unknown	
Quadrupole	10	1.0	
Drift	20		
Quadrupole	20	−1.0	
Drift	20		
Quadrupole	10	1.0	

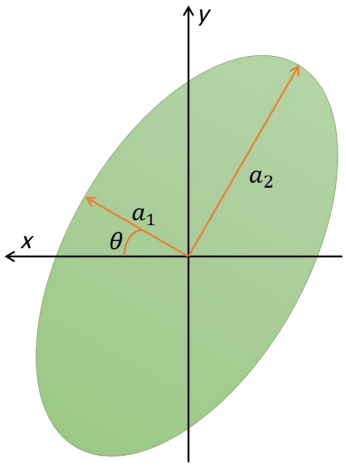

FIG. 2. Ellipse of an x-y coupled beam in real space. A_{xy} is the rms area of the beam, see Eq. (44). Parameters α_{xy} and β_{xy} are its equivalent Twiss parameters defining the ellipse orientation and aspect ratio in real space. The x, y, and s unit vectors of the Cartesian coordinate system follow the right-hand rule.

B. High current case

For KV beams, the electric self-field caused by space charge can be calculated analytically as done by Sacherer [1] for uncoupled beams, i.e., for upright ellipses. In the case of coupling, the ellipse is generally tilted as drawn in Fig. 2. Here, the space charge forces are first calculated within the tilted frame. In the second step, these forces are projected into the upright laboratory frame and applied to the beam. They are equivalent to a defocusing quadrupole kick in both planes. The strengths are not equal along both planes but the resulting 4D transformation is linear and symplectic. Hence it will be modeled by another 4×4 transport matrix $\varkappa$.

The ellipse is described by its two semiaxes a_1 and a_2 and by the rotation angle θ of a_1 with respect to x axis. Its rms area is given by

$$A_{xy} = \sqrt{\langle xx\rangle\langle yy\rangle - \langle xy\rangle^2} = a_1 \cdot a_2. \tag{44}$$

The above ellipse parameters are calculated from the beam second moments through

$$\beta_{xy} = \frac{\langle xx\rangle}{A_{xy}}, \qquad \alpha_{xy} = -\frac{\langle xy\rangle}{A_{xy}}, \tag{45}$$

$$\Theta = \frac{1}{2}\arctan\left(\frac{-2\alpha_{xy}}{\beta_{xy} - \frac{1+\alpha_{xy}^2}{\beta_{xy}}}\right), \quad h = \frac{\beta_{xy}}{2} + \frac{1+\alpha_{xy}^2}{2\beta_{xy}}, \tag{46}$$

and

$$a_{1,2} = \sqrt{\frac{A_{xy}}{2}}(\sqrt{h+1} \pm \sqrt{h-1}). \tag{47}$$

The transport matrix $\varkappa$ is calculated from the ellipse geometric parameters and the general beam parameters as

$$\varkappa = R^{-1}(\Theta) \cdot \varkappa^* \cdot R(\Theta), \tag{48}$$

where $\varkappa^*$ is the matrix in the tilted ellipse frame. It reads

$$\varkappa^*_{1,2} = \begin{bmatrix} 1 & 0 \\ \kappa_{1,2}\delta s & 1 \end{bmatrix}, \qquad \varkappa^* = \begin{bmatrix} \varkappa^*_1 & O \\ O & \varkappa^*_2 \end{bmatrix}, \tag{49}$$

with δs being the step size along s between two space charge kicks. $\kappa_{1,2}$ are the respective kick strengths along each semiaxis and are given by

$$\kappa_1 = \frac{\kappa_{sc}}{2a_1(a_1+a_2)}, \qquad \kappa_2 = \frac{\kappa_{sc}}{2a_2(a_1+a_2)}, \tag{50}$$

from the generalized beam perveance

$$\kappa_{sc} = \frac{qI}{2\pi\epsilon_0 m(\gamma\beta c)^3}, \tag{51}$$

with q as particle charge, I as beam current, and β and γ as relativistic factors.

With these prerequisites, any beam line from (skewed) quadrupoles transporting a coupled intense beam is modeled through a sequence of symplectic linear transport matrices. Quadrupoles and drifts are subdivided into many slices each and transportation through them is by a sequence of transports along slice length δs without space charge and execution of the space charge kick with $\varkappa$ afterward. This method has been implemented into many codes. For uncoupled beams, the PARMILA code [18] for instance uses it to design periodic lattices and to evaluate their performances. Here it shall serve to obtain cell-by-cell periodic solutions for intense coupled beams.

V. PERIODIC SOLUTION OF ONE CELL

Solutions C of the beam matrix along periodic channels are considered periodic if they meet

$$C(s_2) \approx C(s_2 + \ell) \tag{52}$$

to a very good approximation. Section IV A presented such a solution $C^0(s_2)$ for zero current. This solution will not hold with the beam current being switched on. This is from the dependence of the cell transport matrix $\mathfrak{T}$ from the beam current and from the beam Twiss parameters at the entrance to the channel as shown in Sec. IV B.

In order to find a solution that holds even with current, another iterative procedure is applied. It uses the method of determining a matching setting $\aleph$ presented in Sec. IV A.

Additionally, it performs an iterative switching between obtaining the periodic transport matrix from tracking and using it to readapt the matching to it.

The iterative procedure starts from the beam moments matrix $C(s_1)$ behind the solenoid being then transported through the matching line $\mathfrak{R}(\aleph^0)$ for zero current. The resulting beam matrix at the entrance to the channel

$$C^0(s_2) = \mathfrak{R}(\aleph^0) \cdot C(s_1) \cdot \mathfrak{R}^{\mathrm{T}}(\aleph^0), \tag{53}$$

is then tracked with high current ($I = 10$ mA) through one cell. Accordingly, the total transport matrix of the cell $\mathfrak{T}_{\mathrm{sc}}(\aleph^0)$ is a result of the tracking procedure described in Sec. IV B. $\mathfrak{T}_{\mathrm{sc}}(\aleph^0)$ depends on the current I and on the spatial beam parameters at the entrance of the channel. The 4×4 elements of $\mathfrak{T}_{\mathrm{sc}}(\aleph^0)$ are stored for further use. Most likely, $C^0(s_2)$ does not meet the condition of the periodic solution with current, i.e.,

$$C^0(s_2) \neq \mathfrak{T}_{\mathrm{sc}}(\aleph^0) \cdot \mathfrak{R}(\aleph^0) \cdot C(s_1) \cdot \mathfrak{R}^{\mathrm{T}}(\aleph^0) \cdot \mathfrak{T}_{\mathrm{sc}}^{\mathrm{T}}(\aleph^0). \tag{54}$$

However, the cell matrix $\mathfrak{T}_{\mathrm{sc}}(\aleph^0)$ is used to readapt the matching setting such, that a new matching $\aleph^1$ is found which provides for equal beam matrices before and after transport through the cell matrix $\mathfrak{T}_{\mathrm{sc}}(\aleph^0)$

$$C^1(s_2) = \mathfrak{T}_{\mathrm{sc}}(\aleph^0) \cdot \mathfrak{R}(\aleph^1) \cdot C(s_1) \cdot \mathfrak{R}^{\mathrm{T}}(\aleph^1) \cdot \mathfrak{T}_{\mathrm{sc}}^{\mathrm{T}}(\aleph^0), \tag{55}$$

emphasizing that the above equation uses the stored elements of $\mathfrak{T}_{\mathrm{sc}}(\aleph^0)$.

This new matching $\aleph^1$ delivers the beam matrix $C^1(s_2)$ in front of the channel. It is now retracked with current through the cell as described in Sec. IV B. The tracking will provide a new cell matrix $\mathfrak{T}_{\mathrm{sc}}(\aleph^1)$. Again its 4×4 elements are stored to readapt the matching to a setting $\aleph^2$ meeting the periodic solution assuming the new matrix $\mathfrak{T}_{\mathrm{sc}}(\aleph^1)$ along the channel

$$C^2(s_2) = \mathfrak{T}_{\mathrm{sc}}(\aleph^1) \cdot \mathfrak{R}(\aleph^2) \cdot C(s_1) \cdot \mathfrak{R}^{\mathrm{T}}(\aleph^2) \cdot \mathfrak{T}_{\mathrm{sc}}^{\mathrm{T}}(\aleph^1). \tag{56}$$

This in turn provides a new beam matrix $C^2(s_2)$ in front of the channel, which changes the transport matrix of the cell to $\mathfrak{T}_{\mathrm{sc}}(\aleph^2)$. Continuing this procedure finally converges, i.e., the changes from $\aleph^{n-1}$ to $\aleph^n$ become very small and finally negligible. Accordingly, after a sufficient amount of iterations J, the periodic condition is fulfilled through

$$C^J(s_2) \approx \mathfrak{T}_{\mathrm{sc}}(\aleph^J) \cdot \mathfrak{R}(\aleph^J) \cdot C(s_1) \cdot \mathfrak{R}^{\mathrm{T}}(\aleph^J) \cdot \mathfrak{T}_{\mathrm{sc}}^{\mathrm{T}}(\aleph^J). \tag{57}$$

The matrix $C^J(s_2)$ contains the periodic beam moments at the entrance to the channel and $\mathfrak{T}_{\mathrm{sc}}(\aleph^J)$ is the periodic transport matrix of the cell including current and coupling. Since all $\mathfrak{T}_{\mathrm{sc}}(\aleph^n)$ are products from symplectic slice matrices, all matrices $C^n(s_2)$ have the same eigenemittances.

In case of the example presented here, sufficient convergence has been reached at $J = 6$, and the corresponding input beam matrix (in units of mm and mrad) is

$$C^6(s_2) = \begin{bmatrix} +147.8 & +0.006 & +59.34 & -0.006 \\ \cdots & +80.44 & +0.006 & +114.9 \\ \cdots & \cdots & +47.36 & +0.011 \\ \cdots & \cdots & \cdots & +286.7 \end{bmatrix}, \tag{58}$$

with coupling parameter of $t = 1.07$. The corresponding output beam matrix (in units of mm and mrad) is

$$C^6(s_2 + \ell) = \begin{bmatrix} +147.8 & +0.026 & +59.33 & -0.106 \\ \cdots & +80.41 & +0.035 & +114.9 \\ \cdots & \cdots & +47.34 & -0.017 \\ \cdots & \cdots & \cdots & +286.8 \end{bmatrix}, \tag{59}$$

and the according transport matrix along one cell is determined as (in units of m and rad)

$$\mathfrak{T}_{\mathrm{sc}}(\aleph^6) = \begin{bmatrix} +0.452 & +1.254 & -0.091 & -0.016 \\ -0.633 & +0.452 & -0.092 & -0.027 \\ -0.027 & -0.016 & +0.447 & +0.376 \\ -0.092 & -0.091 & -2.125 & +0.447 \end{bmatrix}, \tag{60}$$

with corresponding phase advances of $\mu_x = 63.11°$ and $\mu_y = 63.44°$, respectively. The corresponding beam moments along a channel comprising two cells are plotted in Fig. 3. It shows that the cell-to-cell periodicity of an intense coupled coasting beam can be achieved under the assumption of a KV distribution. Figure 4 plots the six 2D projections of the phase space ellipses in front of and behind the channel.

This section shall be closed by a comparison of the fully 4D-periodic solution along the channel with the one obtained from simple 2D-envelope matching. The latter is state-of-the-art and uses just regular quadrupoles. Accordingly, the details of the latter are not given and just the results shall be reported.

This 2D envelope matching ignores the coupled beam moments leading to the noncoupling matching transfer matrix (in units of m and rad)

$$\mathfrak{R}^{\dagger} = \begin{bmatrix} +0.361 & +1.114 & 0 & 0 \\ -0.829 & +0.211 & 0 & 0 \\ 0 & 0 & +0.035 & +0.613 \\ 0 & 0 & -1.609 & +0.382 \end{bmatrix}. \tag{61}$$

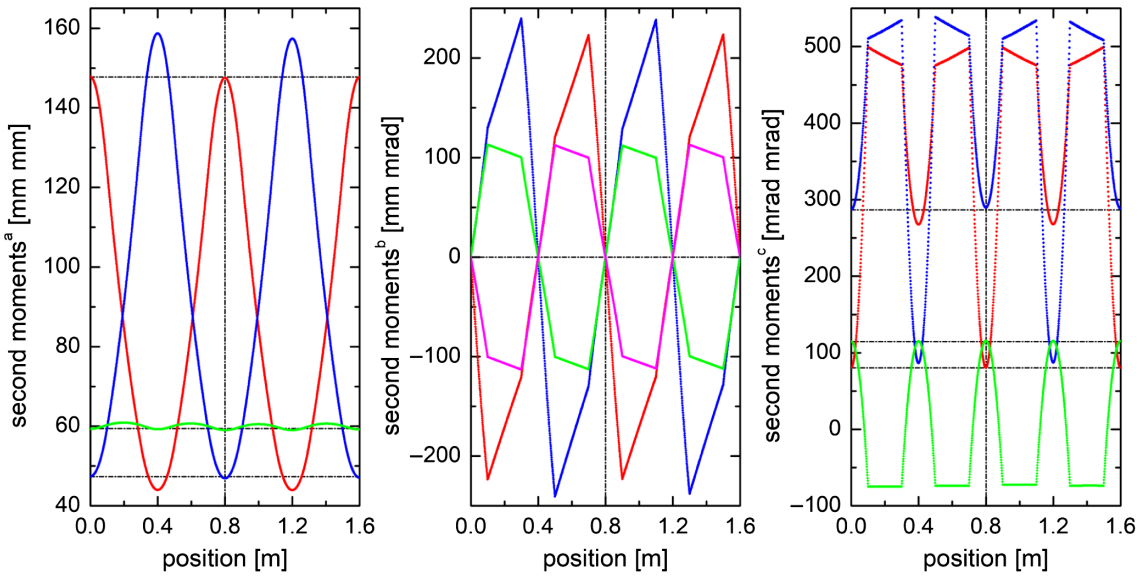

FIG. 3. Full 4D-periodic solution: the ten independent rms moments along the regular quadrupole channel (two cells) for a coupled proton beam with 10 mA. Left: rms moments x_1, y_1, and z_1 (red, blue, and green); Middle: rms moments x_2, y_2, z_2, and z_3 (red, blue, green, and magenta); Right: rms moments x_3, y_3, and z_4 (red, blue, and green).

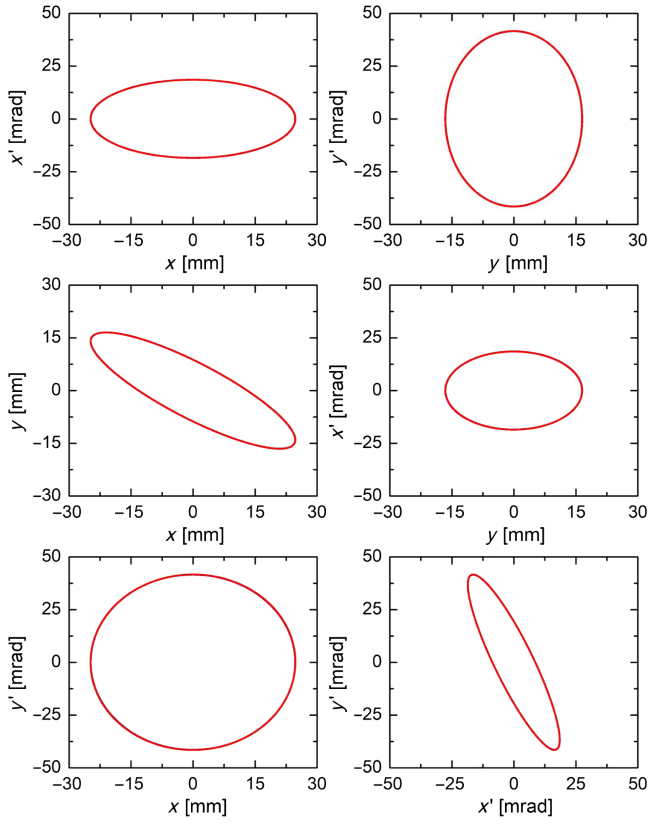

FIG. 4. From full 4D-periodic solution: projected $4 \times$ rms ellipses of the beam second moments matrix at the entrance (blue) and exit (red) of the periodic channel for a coupled proton beam with 10 mA. It is obtained that $C^6(s_2) \approx C^6(s_2 + \ell)$.

The resulting beam matrix at the entrance of the channel is (in units of mm and mrad)

$$C^\dagger(s_2) = \begin{bmatrix} +183.6 & +0.169 & +100.0 & 0 \\ \cdots & +101.1 & 0 & -10.00 \\ \cdots & \cdots & +59.34 & +0.019 \\ \cdots & \cdots & \cdots & +379.7 \end{bmatrix}, \tag{62}$$

while the corresponding beam matrix at the exit is (in units of mm and mrad)

$$C^\dagger(s_2 + \ell) = \begin{bmatrix} +186.1 & +1.967 & +6.026 & -103.7 \\ \cdots & +105.1 & -30.71 & +157.4 \\ \cdots & \cdots & +61.88 & +5.640 \\ \cdots & \cdots & \cdots & +388.7 \end{bmatrix}. \tag{63}$$

Figure 5 compares the six 2D projections of the 4D phase space ellipses $C^\dagger(s_2)$ and $C^\dagger(s_2 + \ell)$ in front of and behind the first cell of the periodic channel. As expected, periodicity is achieved for the horizontal and vertical planes. However, there is no periodicity in the projections that mix the two planes. In the following section, the results from KV-rms-tracking are benchmarked with particle tracking of a beam with Gaussian distribution.

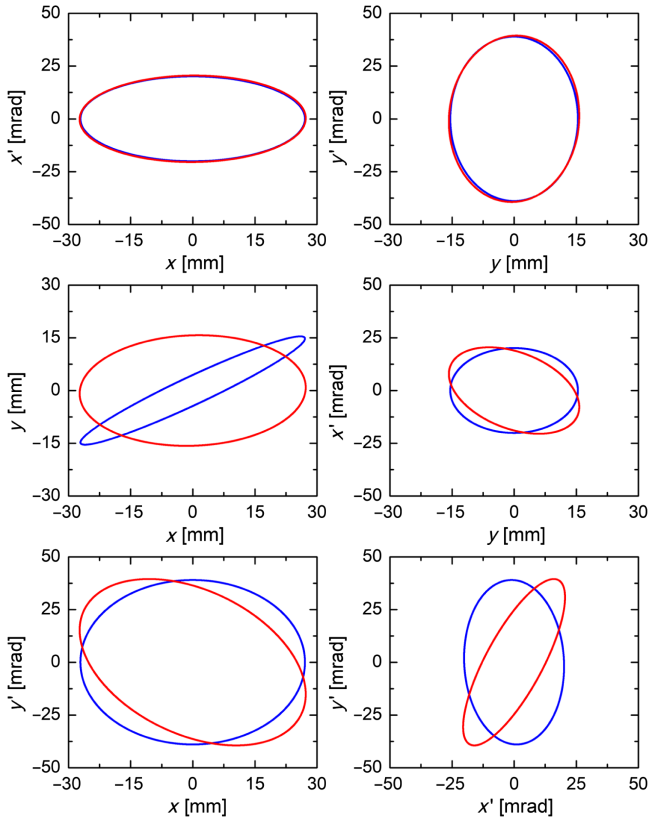

FIG. 5. From 2D-envelope matching: projected 4 × rms ellipses of the beam second moments matrix at the entrance (blue) and exit (red) of the periodic channel for a coupled proton beam with 10 mA.

VI. BENCHMARKING

Benchmarking has been done with MATHCAD using a KV-type beam and BEAMPATH [19] using a Gaussian-type beam. Initial distributions of 2×10^4 particles are rms

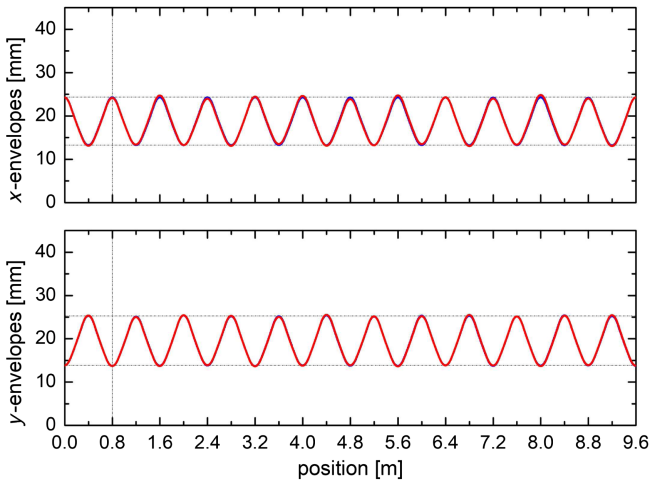

FIG. 6. From full 4D-periodic solution: horizontal and vertical 2 × rms-beam sizes of a coupled 10 mA proton beam along a regular FODO quadrupole channel as obtained from rms tracking (blue) and particle tracking (red). The initial particle distribution is rms equivalent to beam matrix $C^6(s_2)$.

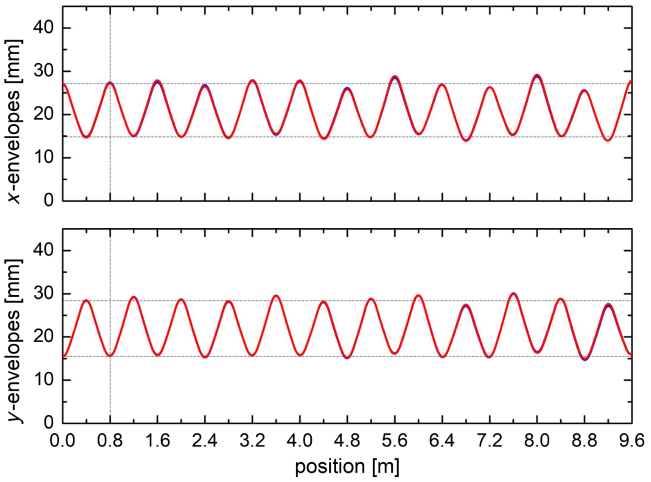

FIG. 7. From 2D-envelope matching: horizontal and vertical 2 × rms-beam sizes of a coupled 10 mA proton beam along a regular FODO quadrupole channel as obtained from rms tracking (blue) and particle tracking (red). The initial particle distribution is rms equivalent to beam matrix $C^\dagger(s_2)$.

equivalent to the second beam moments matrices $C^6(s_2)$ from Eq. (58) and $C^\dagger(s_2)$ from Eq. (62), respectively. Particle-tracking simulations have been done using a 10 mA proton beam and 12 cells of the periodic channel. Figures 6 and 7 show the transverse 2 × rms-beam sizes along the quadrupole channel obtained from rms tracking described in Sec. IV B and extracted from particle tracking simulation with BEAMPATH.

Applying cell-to-cell second moments matching, both, transverse 2 × rms-beam sizes from KV-rms tracking and from particle tracking a Gaussian beam, reveal a high degree of envelope matching to the lattice periodicity.

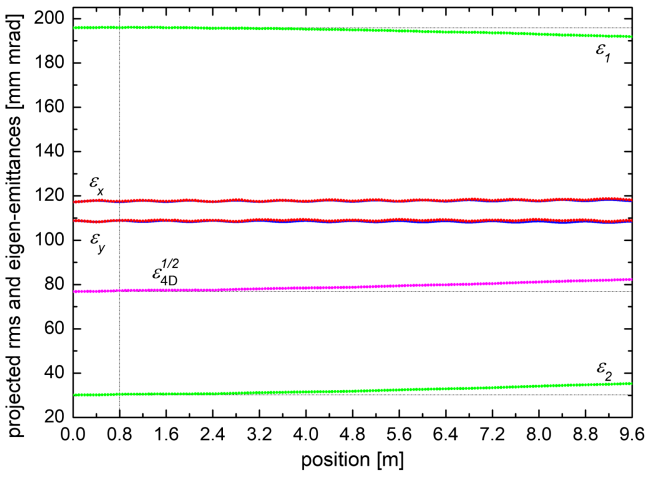

FIG. 8. From full 4D-periodic solution: transverse projected rms emittances as obtained from rms tracking (blue) and particle tracking (red). Green (magenta) curves indicate the eigenemittances (square roots of the 4D emittances) calculated from particle tracking. The initial particle distribution is rms equivalent to beam matrix $C^6(s_2)$.

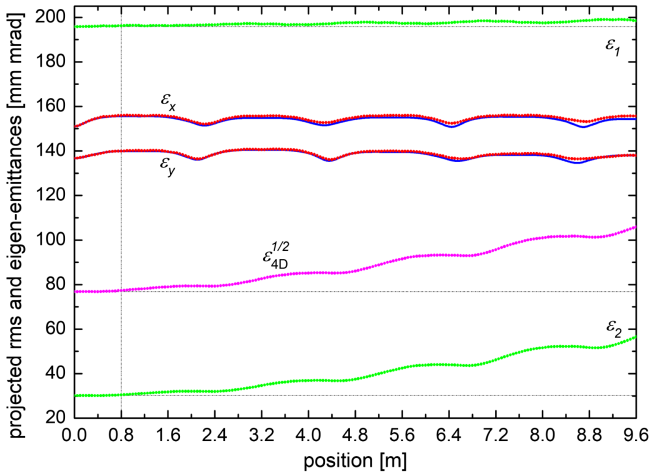

FIG. 9. From 2D-envelope matching: transverse projected rms emittances as obtained from rms tracking (blue) and particle tracking (red). Green (magenta) curves indicate the eigenemittances (square roots of the 4D emittances) calculated from particle tracking. The initial particle distribution is rms equivalent to beam matrix $C^{\dagger}(s_2)$.

The KV-based rms-beam size is very regular and the Gaussian rms-beam size shows slight fluctuation. Those are to be expected since space charge forces especially at the outer parts of the beam are different for KV and for Gaussian distributions. The matching proofed to work very well even for the Gaussian beam. Applying simple 2D-envelopes matching, the transverse $2\times$ rms-beam sizes are still well matched with the periodic quadrupole channel, although the fluctuations are notably larger compared to those of the full 4D solution.

Eigenemittances are preserved by symplectic transformations as KV-rms tracking. Instead, nonlinear space charge forces occurring at particle tracking of a Gaussian beam do not preserve the eigenemittances. Figures 8 and 9 plot

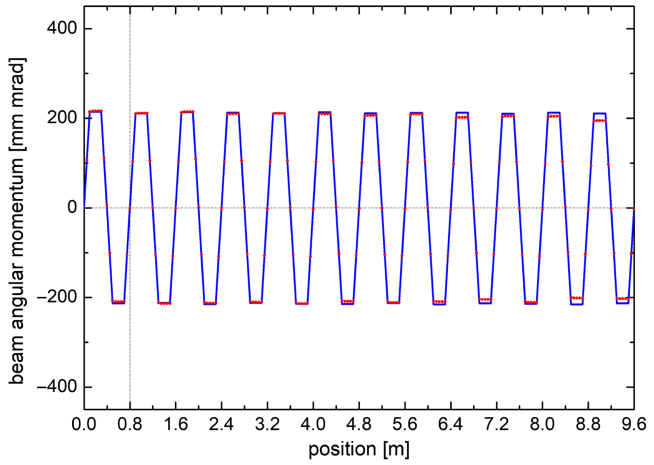

FIG. 10. From full 4D-periodic solution: angular momentum as obtained from rms tracking (blue) and particle tracking (red). The initial particle distribution is rms equivalent to beam matrix $C^{6}(s_2)$.

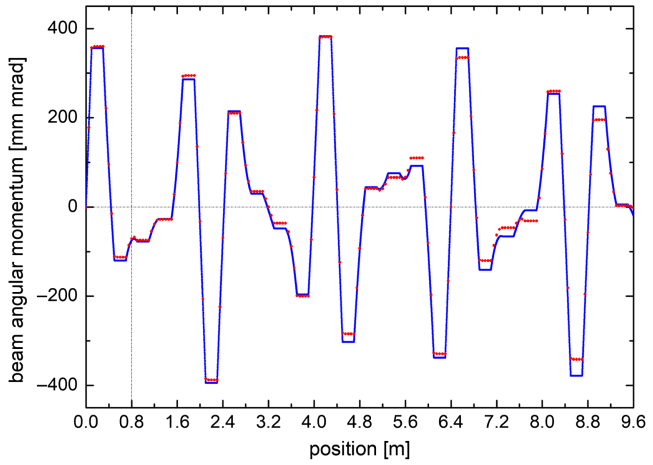

FIG. 11. From 2D-envelope matching: angular momentum as obtained from rms tracking (blue) and particle tracking (red). The initial particle distribution is rms equivalent to beam matrix $C^{\dagger}(s_2)$.

eigenemittances, projected rms emittances, and square roots of 4D emittances along the channel from particle-tracking simulations.

Beam transport along the channel applying the full 4D-periodic solution results in a total growth of the 4D emittance of 15%. If instead the simple 2D-envelope matched transport is used, the corresponding growth is 90%. This provides for strong evidence, that full 4D-periodic transport has strong advantages compared to simple 2D matching in case of a coupled beam. For completion, Figs. 10 and 11 plot the beam angular momentum along the channel as obtained from the full 4D-periodic solution and 2D-envelope matching.

VII. CONCLUSION

It has been shown that a cell-to-cell full 4D-periodic solution can be determined for a coupled beam with considerable space charge forces. This has been accomplished by rms tracking of coupled beams with KV distribution combined with a dedicated iterative procedure of tracking and generic rematching. Benchmarking with an initial Gaussian distribution along a channel with a large cell number revealed that the method works very well. Hence, it provides a tool for systematic investigations of intense, coupled beam transport along periodic lattices. Full 4D periodicity of the beam revealed to suppress the growth of the 4D emittance much better with respect to simple 2D-envelope matching. One special application for 4D periodicity is imposing well-defined angular momentum to beams being transported along such lattices as drift tube linacs for instance.

APPENDIX: TRANSFER MATRICES OF MATCHING SECTION

For high current beam injection into the channel, the zero current transfer matrix of the matching section $\mathfrak{R}(\aleph^0)$ has

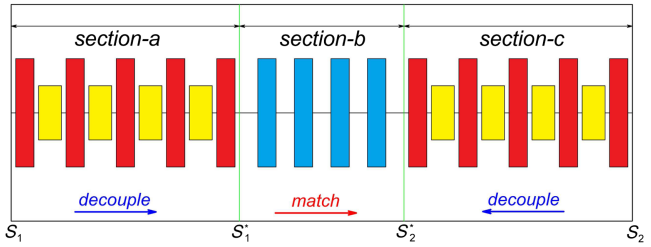

FIG. 12. Conceptual matching beam line includes the rotated quadrupoles (red blocks), solenoids (yellow blocks), and regular quadrupoles (blue blocks).

been used as the initial transfer matrix and the optimization routine has been applied again giving (in units of m and rad)

$$\mathfrak{R}(\aleph^5) = \begin{bmatrix} +1.048 & +1.153 & +0.620 & -1.553 \\ -0.036 & +0.325 & +0.268 & +0.325 \\ +0.119 & -0.842 & +0.434 & +0.558 \\ +0.664 & +0.499 & -0.129 & +0.713 \end{bmatrix}, \quad \text{(A1)}$$

satisfying Eq. (57) and

$$C^6(s_2) = \mathfrak{R}(\aleph^5) \cdot C(s_1) \cdot \mathfrak{R}^{\mathrm{T}}(\aleph^5). \quad \text{(A2)}$$

As mentioned previously, the detailed provision of the 4D-matching beam line is a hard task being beyond the scope of this paper. However, this section shall sketch a conceptual approach to obtain an according layout. It is drawn schematically in Fig. 12 and it comprises three sections.

Sections-a and c each comprise five rotated quadrupoles being separated by solenoids. Within these sections, the beam is coupled. Section-b in between comprises just four regular quadrupoles and the beam along this section is fully decoupled.

Provision of the full matching beam line starts with the determination of the settings of section-c. It uses the known periodic solution with space charge at the beginning of the periodic channel at position s_2. Its according beam moments matrix $C^6(s_2)$ is transported backward to position s_2^*. This backward transportation is done such that the resulting beam is fully decoupled at s_2^*. The required settings are denoted as $\S^c$ and they comprise the quadrupole strengths, rotation angles, and solenoid strengths. These parameters are obtained through an appropriate numerical routine (*Minimize* of MATHCAD for instance). The according backward transport matrix is denoted as $\mathfrak{R}_c^{-1}$.

Within the second step, the settings of section-a are determined numerically in order to decouple the beam at the coupling production section's exit at position s_1. The according transport matrix is denoted as $\mathfrak{R}_a$ and it provides for the decoupled beam at position s_1^*. Its settings are summarized as $\S^a$. Finally, the matching beam line is completed by an appropriate section-b modeled by the transport matrix $\mathfrak{R}_b$, which just provides for the matching between the two uncoupled beam matrices at s_1^* and s_2^*. The transport matrix of the complete matching line hence reads as

$$\mathfrak{R} = \mathfrak{R}_c \cdot \mathfrak{R}_b \cdot \mathfrak{R}_a, \quad \text{(A3)}$$

and accordingly

$$C^6(s_2) = \mathfrak{R}_c \cdot \mathfrak{R}_b \cdot \mathfrak{R}_a \cdot \wp \cdot C(s_0) \cdot \wp^{\mathrm{T}} \cdot \mathfrak{R}_a^{\mathrm{T}} \cdot \mathfrak{R}_b^{\mathrm{T}} \cdot \mathfrak{R}_c^{\mathrm{T}}, \quad \text{(A4)}$$

15 rotated quadruples, 4 regular quadrupoles, and 12 solenoids are needed totally.

An alternative beam line may just apply section-c to replace the coupling section and matching section

$$C^6(s_2) = \mathfrak{R}_c \cdot C(s_2^*) \cdot \mathfrak{R}_c^{\mathrm{T}}, \quad \text{(A5)}$$

requiring just five rotated quadrupoles and four solenoids (coupling section and section-a and b are not needed). It corresponds to (in units of m and rad)

$$\mathfrak{R}_c = \begin{bmatrix} -0.122 & +2.338 & +0.414 & +1.280 \\ -0.245 & +0.419 & -0.401 & -0.086 \\ +0.064 & -1.225 & +0.237 & +0.734 \\ +0.428 & -0.730 & -0.765 & -0.164 \end{bmatrix}, \quad \text{(A6)}$$

and the parameters of this alternative beam line (section-c) are listed in Table III. It is emphasized that the quadrupole magnets in this section must be individually rotatable

TABLE III. Parameters of the alternative beam line (section-c). The unit of the solenoid field is T.

Elements	'Length (cm)	Strength (T/m)	Rotation (°)
Drift	5		
Rotated quad	20	0.136	11.53
Drift	5		
Solenoid	25	0.075	
Drift	5		
Rotated quad	20	−0.022	−9.390
Drift	5		
Solenoid	25	0.075	
Drift	5		
Rotated quad	20	−0.155	3.462
Drift	5		
Solenoid	25	0.075	
Drift	5		
Rotated quad	20	−0.046	−5.477
Drift	5		
Solenoid	25	0.075	
Drift	5		
Rotated quad	20	0.105	2.487
Drift	5		

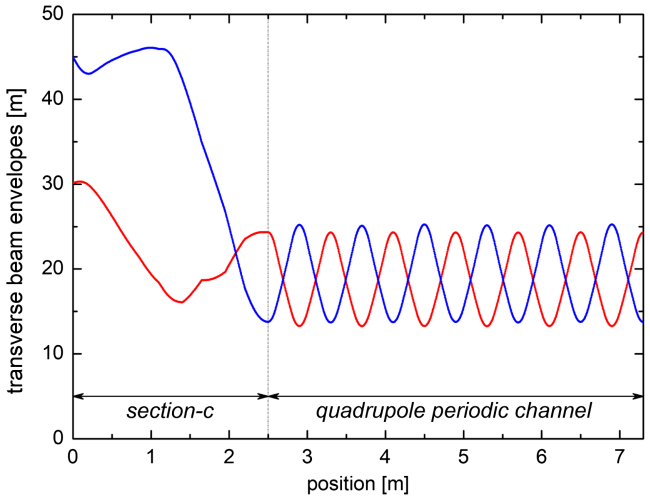

FIG. 13. Horizontal (red) and vertical (blue) $2\times$ rms-beam sizes along the alternative beam line (section-*c*) and six cells of the quadrupole periodic channel.

to adapt the line to input beam matrices with different amounts of coupling according to different amounts of angular momentum for instance. Corresponding transverse $2\times$ rms-beam sizes are shown in Fig. 13.

[1] F. Sacherer, RMS envelope equations with space charge, IEEE Trans. Nucl. Sci. **18**, 1105 (1971).

[2] T. P. Wangler, *RF Linear Accelerators*, 2nd ed. (Wiley-VCH, Mannheim/Germany, 2008), p. 296.

[3] L. Groening, W. Barth, W. Bayer, G. Clemente, L. Dahl, P. Forck, P. Gerhard, I. Hofmann, G. Riehl, and S. Yaramyshev, Benchmarking of measurement and simulation of transverse rms-emittance growth, Phys. Rev. ST Accel. Beams **11**, 094201 (2008).

[4] L. Groening, M. Maier, C. Xiao, L. Dahl, P. Gerhard, O. K. Kester, S. Mickat, H. Vormann, M. Vossberg, and M. Chung, Experimental proof of adjustable single-knob ion beam emittance partitioning, Phys. Rev. Lett. **113**, 264802 (2014).

[5] Dong-O Jeon, Experimental evidence of space charge driven resonances in high intensity linear accelerators, Phys. Rev. Accel. Beams **19**, 010101 (2016).

[6] M. Reiser, *Theory and Design of Charged Particle Beams* (John Wiley & Sons Inc., New York, 1994).

[7] Linac4 Technical Design Report, edited by F. Gerigk and M. Vretenar, CERN, Geneva Report No. CERN-AB-2006-084-ABP/RF, 2006.

[8] R. Friehmelt, Dimensionierung der Quadrupolfokussierung in einem Schwerionen-Linearbeschleuniger, UNILAC Bericht Nr. 5-67, Universität Heidelberg, 1967.

[9] Yoo-Lim Cheon, Seok-Ho Moon, and Moses Chung, Effects of beam spinning on the fourth-order particle resonance of 3D bunched beams in high-intensity linear accelerator, Phys. Rev. Accel. Beams **25**, 064002 (2022).

[10] A. Khan, O. Boine-Frankenheim, F. Hug, and C. Stoll, Beam matching with space charge in energy recovery linacs, Nucl. Instrum. Methods Phys. Res., Sect. A **948**, 162822 (2019).

[11] J. J. Barnard and B. Losic, Envelope modes of beams with angular momentum, in *Proceedings of the 20th International Linac Conference, LINAC-2000, Monterey, CA, 2000* (SLAC, Menlo Park, CA, 2000).

[12] A. Hoover, N. J. Evans, and J. A. Holmes, Computation of the matched envelope of the Danilov distribution, Phys. Rev. Accel. Beams **24**, 044201 (2021).

[13] D. Chernin, Evolution of rms beam envelopes in transport systems with linear *x*-*y* coupling, Part. Accel. **24**, 29 (1988), http://cds.cern.ch/record/1053510/files/p29.pdf.

[14] K. R. Crandall and D. P. Rusthoi, Documentation for TRACE: An interactive beam-transport code, Los Alamos National Laboratory, Internal Report No. LA-10235-MS, 1985.

[15] R. A. Kishek, J. J. Barnard, and D. P. Grote, Effects of quadrupole rotations on the transport of space-charge-dominated beams: theory and simulations comparing linacs with circular machines, in *Proceedings of the 1999 Particle Accelerator Conference (PAC'99), New York, 1999* (IEEE, New York, 1999), pp. 1761–1763, https://ieeexplore.ieee.org/stamp/stamp.jsp?tp=&arnumber=794251.

[16] C. Xiao, M. Maier, X. N. Du, P. Gerhard, L. Groening, S. Mickat, and H. Vormann, Rotating system for four-dimensional transverse rms-emittance measurements, Phys. Rev. Accel. Beams **19**, 072802 (2016).

[17] PTC Mathcad, https://www.ptc.com/en/engineering-math-software/mathcad.

[18] J. H. Billen and H. Takeda, PARMILA Manual, Report No. LAUR-98-4478, Los Alamos, 1998 (Revised 2004).

[19] Y. K. Batygin, Particle-in-cell code BEAMPATH for beam dynamics simulations in linear accelerators and beam lines, Nucl. Instrum. Methods Phys. Res., Sect. A **539**, 455 (2005).